

# **SANDIA REPORT**

SAND2006-4359

Unlimited Release

Printed August 2006

## **Improved InGaN Epitaxy Yield by Precise Temperature Measurement: Yearly Report 1**

J. Randall Creighton, Daniel D. Koleske, Michael J. Russell, and Arthur J. Fischer

Prepared by  
Sandia National Laboratories  
Albuquerque, New Mexico 87185 and Livermore, California 94550

Sandia is a multiprogram laboratory operated by Sandia Corporation,  
a Lockheed Martin Company, for the United States Department of Energy's  
National Nuclear Security Administration under Contract DE-AC04-94AL85000.

Approved for public release; further dissemination unlimited.



**Sandia National Laboratories**

Issued by Sandia National Laboratories, operated for the United States Department of Energy by Sandia Corporation.

**NOTICE:** This report was prepared as an account of work sponsored by an agency of the United States Government. Neither the United States Government, nor any agency thereof, nor any of their employees, nor any of their contractors, subcontractors, or their employees, make any warranty, express or implied, or assume any legal liability or responsibility for the accuracy, completeness, or usefulness of any information, apparatus, product, or process disclosed, or represent that its use would not infringe privately owned rights. Reference herein to any specific commercial product, process, or service by trade name, trademark, manufacturer, or otherwise, does not necessarily constitute or imply its endorsement, recommendation, or favoring by the United States Government, any agency thereof, or any of their contractors or subcontractors. The views and opinions expressed herein do not necessarily state or reflect those of the United States Government, any agency thereof, or any of their contractors.

Printed in the United States of America. This report has been reproduced directly from the best available copy.

Available to DOE and DOE contractors from  
U.S. Department of Energy  
Office of Scientific and Technical Information  
P.O. Box 62  
Oak Ridge, TN 37831

Telephone: (865) 576-8401  
Facsimile: (865) 576-5728  
E-Mail: [reports@adonis.osti.gov](mailto:reports@adonis.osti.gov)  
Online ordering: <http://www.osti.gov/bridge>

Available to the public from  
U.S. Department of Commerce  
National Technical Information Service  
5285 Port Royal Rd.  
Springfield, VA 22161

Telephone: (800) 553-6847  
Facsimile: (703) 605-6900  
E-Mail: [orders@ntis.fedworld.gov](mailto:orders@ntis.fedworld.gov)  
Online order: <http://www.ntis.gov/help/ordermethods.asp?loc=7-4-0#online>



SAND2006-4359  
Unlimited Release  
Printed August 2006

# Improved InGaN Epitaxy Yield by Precise Temperature Measurement: Yearly Report 1

J. Randall Creighton, Daniel D. Koleske, and Michael J. Russell  
Advanced Materials Sciences Department

Arthur J. Fischer  
Semiconductor Material & Device Sciences Department

Sandia National Laboratories  
P.O. Box 5800  
Albuquerque, NM 87185-1086

## Abstract

This Report summarizes the first year progress (October 1, 2004 to September 30, 2005) made under a NETL funded project entitled "Improved InGaN Epitaxy Yield by Precise Temperature Measurement". This Project addresses the production of efficient green LEDs, which are currently the least efficient of the primary colors. The Project Goals are to advance IR and UV-violet pyrometry to include real time corrections for surface emissivity on mutliwafer MOCVD reactors. Increasing wafer yield would dramatically reduce high brightness LED costs and accelerate the commercial manufacture of inexpensive white light LEDs with very high color quality. This work draws upon and extends our previous research (funded by DOE) that developed emissivity correcting pyrometers (ECP) based on the high-temperature GaN opacity near 400 nm (the ultraviolet-violet range, or UVV), and the sapphire opacity in the mid-IR (MIR) near 7.5 microns

(blank page)

## Contents

1. Introduction.....	7
2. Pyrometry Optics for the Veeco D-125 MOCVD Reactor .....	8
3. Hardware Modifications to the Veeco D-125 MOCVD Reactor .....	9
4. Data Acquisition System (DAQ) .....	13
5. UVV-ECP System Performance .....	13
6. Status of the MIR-ECP System .....	17
7. Milestone Summary .....	19
8. References .....	20

## NOMENCLATURE

DAQ	data acquisition
DOE	Department of Energy
ECP	emissivity correcting pyrometer
IR	infrared
LED	light emitting diode
MIR	mid-infrared
MOCVD	metal organic chemical vapor deposition
NETL	National Energy Technology Laboratory
rms	root mean square
UVV	ultraviolet-violet

# 1. Introduction

Surface temperature measurement during AlGaInN MOCVD is particularly difficult because the epilayers and substrates (typically sapphire) are transparent at the near-IR wavelengths normally used for pyrometry. One solution is to detect radiation near 400 nm (UV-violet range, or UVV) where the GaN epilayers are opaque at the high temperatures encountered during deposition. A method of emissivity-correction should also be applied to improve the utility and accuracy of pyrometry. In fact, emissivity-correction is almost always necessary due to the optical interference effects that occur during heteroepitaxy. Our “standard” method of measuring emissivity is shown in Fig. 1. A modulated light source is used to measure the sample reflectance (R) at the same optical configuration that we are measuring thermal emission. For a specular and opaque surface, the sample emissivity ( $\epsilon$ ) is simple given by Kirchhoff’s relationship;  $\epsilon = 1-R$ .

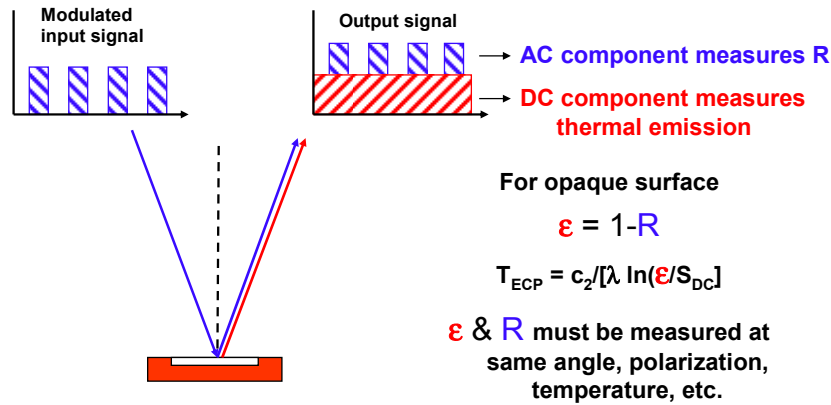


Fig. 1. Schematic of our “standard” emissivity-correction method that measures sample reflectance and thermal emission simultaneously

We previously developed and installed a 1<sup>st</sup> generation UVV emissivity-correcting pyrometer (ECP) on our research MOCVD reactor (CVD1) [1]. The effective wavelength of this system was 405 nm. Overall performance was excellent, with RMS noise levels well below 0.1°C during the 1050°C GaN deposition step. Simultaneous reflectance measurements [2] yield the growth rate, the high-temperature optical constants for GaN, and demonstrate that the epilayer is indeed opaque (once 0.5-1.0 micron of GaN has been deposited). The system was also configured to simultaneously measure reflectance and thermal emission signals at 550 nm. The 550 nm wavelength is useful for monitoring growth rates (from the reflectance signal) over long time spans. Temperature measurements at this wavelength, however, are not reliable due to the transparency of the substrate and epilayers.

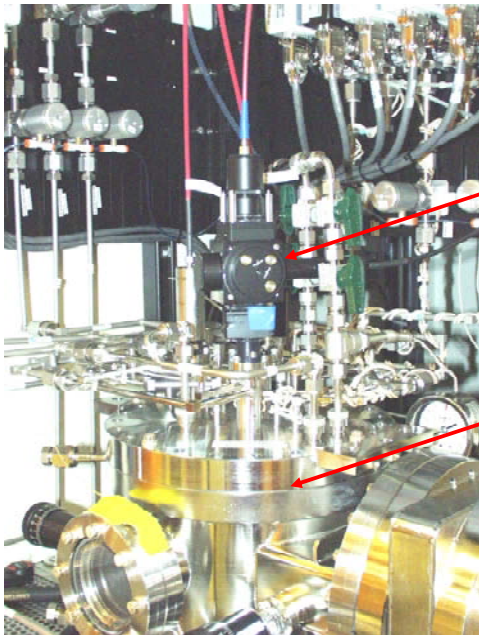
One primary goal of this project was to modify and transfer the UVV-ECP technology to one of our commercial Veeco (formerly Emcore) D-125 MOCVD system. This transfer required significant modifications because the D-125 is a 3-wafer system. A method of synchronizing the detection system with the wafer platen was developed so signals only from the desired wafer(s) could be measured, while rejecting signals from the platen. The D-125 also has more limited optical access, in comparison to CVD1, so the front end optics needed a redesign and optimization.

## 2. Pyrometry Optics for the Veeco D-125 MOCVD Reactor

One challenge is to maximize optical throughput in the more restricted geometry of the D-125 reactors. In our research reactor (CVD1) we were able to use a near normal incidence angle (2-4°) geometry, where the input optics for the reflectance signal are completely separate from the collection optics. In this configuration, no beam-splitter is required, and the stray reflection signal from the top window can typically be entirely rejected spatially. For the D-125 reactors we are forced to adapt a collinear configuration using a beam-splitter, due to the smaller available viewport. The collection/injection optics are mounted on a small reactor viewport (see Fig. 2), and are connected to the detector and reflectance source with fiberoptic cables. In this configuration sizeable reflection signal from the reactor window is detected, and must be accounted for when computing the wafer reflectance. We have chosen a 70T/30R (70% transmittance, 30% reflectance) beam-splitter as a compromise between thermal emission throughput and reflectance signal throughput. The presence this beam-splitter reduces our thermal emission signal by a factor of  $\sim 0.7$  relative to near-normal incidence configuration.

Another significant loss of signal occurs because the relatively small window diameter (16.7 mm) forces us to reduce the collection lens diameter from 23 mm to 15 mm. There is also an aperture in the cold plate (15 mm diameter) about half way to the wafer we account for. The collection lens is the solid angle defining aperture in this system, so the lens diameter reduction alone would reduce the signal by  $\sim 2.4$  X. We can regain some signal by reducing the focal length from 35 mm to 30 mm, which increases the detection solid angle (and the image size on the wafer). In the current version of the system the fiber is positioned to yield an image diameter of 13.5-14 mm on the wafer.

After taking into account the signal loss due the beam-splitter transmission and reduced solid angle, we expect an overall signal reduction of 2.5-2.9 X. The system was calibrated using a blackbody source and compared to the previous UVV-ECP response curve for our single-wafer system. The two calibration curves have the same functional form (i.e. effective wavelength), as expected. The measured D-125 multiwafer system response is 2.6 X smaller than the single wafer system response, in good agreement with our expectations. The magnitude of this signal loss is not of much consequence at high temperatures ( $\sim 1000^\circ\text{C}$ ) where we have abundant signal, but in the 700-800°C range it certainly makes measurements more difficult. Another important signal loss component is the reduced signal duty cycle in a multiwafer system.



System measures Refl and Temp at 405 nm and 550\* nm for each wafer

UVV ECP  
collection/injection optics

Veeco D-125 chamber

\*at 550 nm the wafer is transparent but  
this wavelength is useful for growth rate  
measurements

Fig. 2. NUV-ECP collection/injection optics mounted on Veeco D-125 MOCVD system

### 3. Hardware modifications to the Veeco D-125 MOCVD Reactor

In order to adapt the UVV-ECP to a multiwafer environment (3-2" wafers in this case), a method of synchronizing the data acquisition (DAQ) system with the rotation of the wafer platen must be developed. The goal is to collect data (reflectance and temperature) only from the wafers, while rejecting the signal from the platen. The configuration of the wafers on the platen is shown in Fig. 3. We also need a method a method for indexing the signals, so we can relate the signals to a specific wafer.

The two Sandia Veeco D-125 reactors have somewhat different rotating shaft and platen configurations. Dan Koleske's reactor (DNZ) has a solid rotating shaft machined from a single piece of titanium-zirconium-molybdenum (TZM) alloy. This configuration makes it difficult and relatively expensive to make modifications to DNZ. The end of the DNZ shaft is machined into a conical shape, which mates into a complementary hole in the bottom of the DNZ platen. Andy Allerman's reactor (GNC) has a rotating shaft with a smaller removable tip (referred to as the arbor), which makes reactor modifications somewhat easier. Because of the ease in removing and modifying the arbor we decided to use the GNC-type hardware. For programmatic reasons we decided to add this new hardware to Koleske's reactor (DNZ). A 2<sup>nd</sup> GNC-type shaft was ordered from Veeco, and a modified arbor was designed and constructed to mate with the DNZ platens (see Fig. 4).

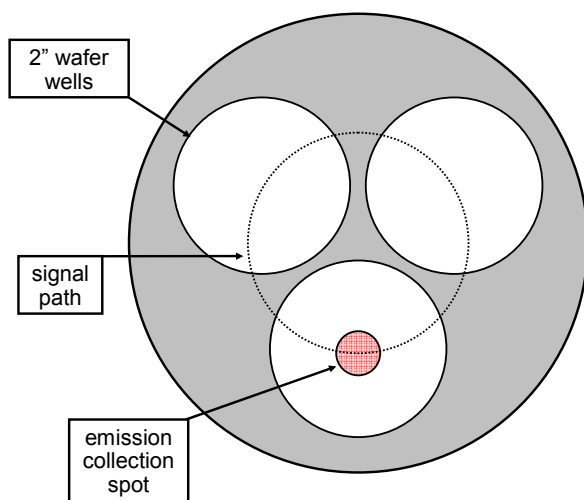


Fig. 3. Schematic of D-125 platen, top-view.

In both GNC and DNZ the platen is actually free to rotate about the shaft, with only friction preventing this movement. During rapid deceleration/acceleration this slippage can be rather severe and is easily observable. The amount of slippage (if any) occurring at steady state conditions varied considerably from run-to-run. Platen-shaft slippage creates a non-trivial signal synchronization and indexing problem. We needed to develop a method of preventing this free rotation, while still allowing for easy loading and removal of the platen (the wafer loading procedure involves transferring the entire platen from the load-lock to the reactor chamber). Our design is based on a “pin-and-slot” concept, shown in Fig. 4. A .040” diameter molybdenum wire (or pin) is inserted into holes drilled in the platen. A complementary slot is machined into the TZM arbor. During platen loading it is necessary to pre-align the shaft in order to mate with the pin in the platen. This adds some complexity to the wafer loading process, but after some adjustments the process has gone smoothly in most cases. Due to problems with the hardware in early stages of development, we ran with an “unpinned” platen during the March-April timeframe. About half of the runs showed little or no slipping. Despite these problems we were able to demonstrate that the UVV-ECP system was working, and Milestone 1.11 was met in March 2005.

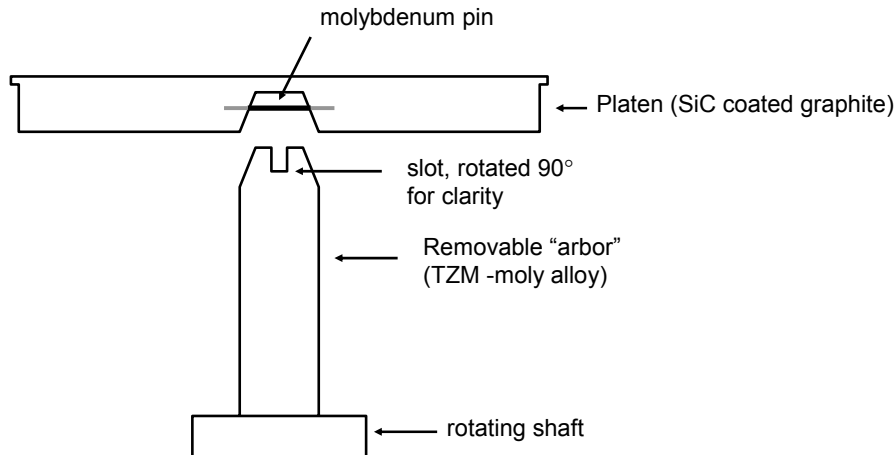


Fig. 4. Hardware “pin-and-slot” method of locking DNZ-type platens to rotating shaft

With the platen no longer free to rotate with respect to the main shaft, we attached an encoding mechanism to the portion of the shaft that protrudes outside the reactor chamber. A small external encoding wheel was fabricated and mounted to the end of the rotating shaft. The wheel has three equally spaced slots that correspond to wafer locations on the platen, and correspond to the Gate Signal (see Fig. 5). A single smaller notch on the edge of the wheel generates a Hardware Trigger that is used to differentiate the three wafer signals.

Another factor to be considered is the duty cycle of the wafer signal. The fraction of the signal path in Fig. 3 that intersects the three wafers is equal to 0.80. However, we cannot use an 80/20 duty cycle (80% on, 20% off) because of the finite size of the emission (and reflectance) collection spot. The effect of the spot size is illustrated in the idealized  $R(550)$  curve in Fig. 5. This is the expected reflectance signal at 550 nm when three specular wafers are loaded on the platen. The platen is a diffuse reflector, so it yields a near zero signal. When the collection spot is entirely on the wafer a constant signal intensity is observed. The trapezoidal shape of the waveform is produced when the collection spot overlaps the wafer and platen. In order to ensure we only detect signal when our collection area (~14 mm diameter) is **entirely** on a wafer we must use a ~55/45 duty cycle (instead of 80/20). The Gate Signal in Fig. 5 illustrates a 55/45 duty cycle.

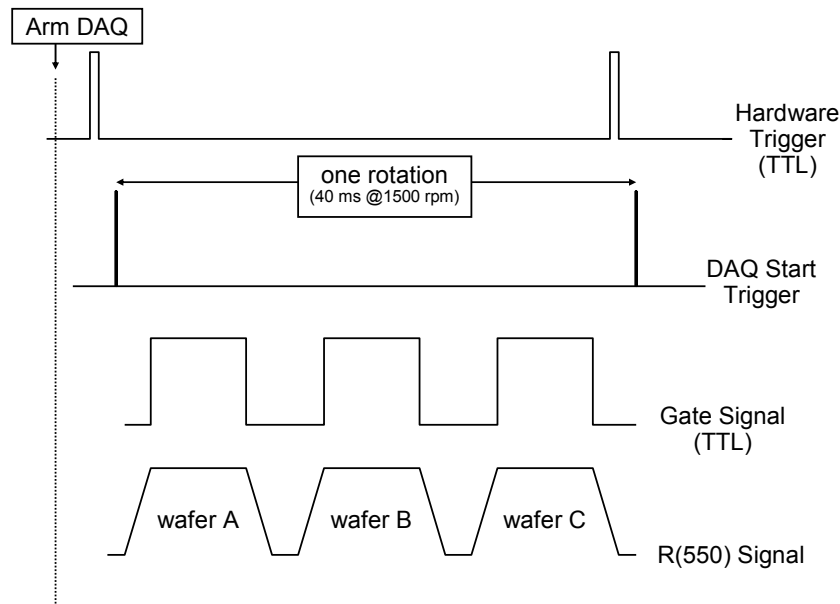


Fig. 5. Timing diagram

The 55/45 duty cycle means we are losing almost a factor of 2 in signal collection time relative to our single wafer MOCVD system. Combined with the 2.6 X loss in optical throughput described in Section 1.1, we have lost a factor of 4.7 X by going to the D-125 system. This also assumes we have three equivalent wafers loaded and are able to signal average all wafers. If we choose to examine only one wafer, we lose another factor of 3.

One other important MOCVD reactor modification we made was shielding the UVV-ECP from the extraneous radiation from the extremely hot rhenium filaments below the platen that serve as the primary heat source. These filaments are estimated to reach temperatures of  $>1400^{\circ}\text{C}$ , and generate copious amounts of  $\sim 400$  nm radiation that scatter around in the main chamber and can possibly corrupt the pyrometer measurements. By adding a short cylindrical radiation shield around the platen we have considerably attenuated the amount of stray light leakage.

In May of 2005 we installed the 1<sup>st</sup> version made from a thin molybdenum foil. Initial results looked very promising, with a dramatic reduction in stray light. The shield also cut the power requirements of the outer filament by 25%, with a 5% reduction on the inner filament. Unfortunately after a week of operation the molybdenum foil lost mechanical integrity and shorted out the outer filament. This required removal of the foil and repair of the filament. In June we installed a 2<sup>nd</sup> version of the radiation shield. This shield is made of TZM (a molybdenum alloy), which has higher temperature integrity, and is significantly thicker (0.016") than the 1<sup>st</sup> shield. The new shield has operated for several months with no sign of failure. This shield still has a small degree of light leakage and might undergo another round of design in the future. Despite some light leakage, the shield has made a significant improvement in pyrometer performance, especially below  $750^{\circ}\text{C}$ . We have not yet quantified the stray light component, but now it appears to be insignificant except during rapid temperature rises when the outer heater filament is running at high current.

## 4. Data Acquisition System (DAQ)

The DAQ code was written in Visual Basic and made considerable use of NI-ComponentWorks controls, graphics, and DAQ objects. One major hurdle in developing this application was maintaining a high software duty cycle efficiency. The total software overhead time (e.g. configuring DAQ boards, reading board signals, number crunching, updating graphics, saving data) needs to be small compared to data collection time. The minimum time to perform a complete DAQ software cycle was empirically determined to be in the 50-100 ms range. One platen rotation at 1500 rpm takes 40 ms (see Fig. 5). If we wrote the code to collect and analyze the signal after only one rotation we would miss the next 2 or 3 rotations due to the software overhead time, yielding a duty cycle efficiency of 25-33%. After considerable investment in time we developed a method of collecting data uninterrupted over multiple rotations (e.g. >10), which involve buffering the intermediate output. With this method we can achieve software duty cycle efficiencies of 0.8-0.9 at reasonable platen integration values (7-20 revolutions).

## 5. UVV-ECP System Performance

A test of the 550 nm reflectance performance during a standard GaN on sapphire recipe with three wafers loaded is shown in Fig. 6. The optical waveforms represent a standard low temperature GaN buffer layer (~30 nm) deposition followed by high temperature GaN deposition (a few microns). The reflectance waveform during the early stages of growth is typically used as a “fingerprint” and used to qualitatively judge of the optimal GaN growth conditions. Each wafer exhibits nearly identical waveforms, but slight differences due to film non-uniformities can be detected. By keeping track of the order of the wafers loaded into the platen, we can relate each waveform to a specific wafer.

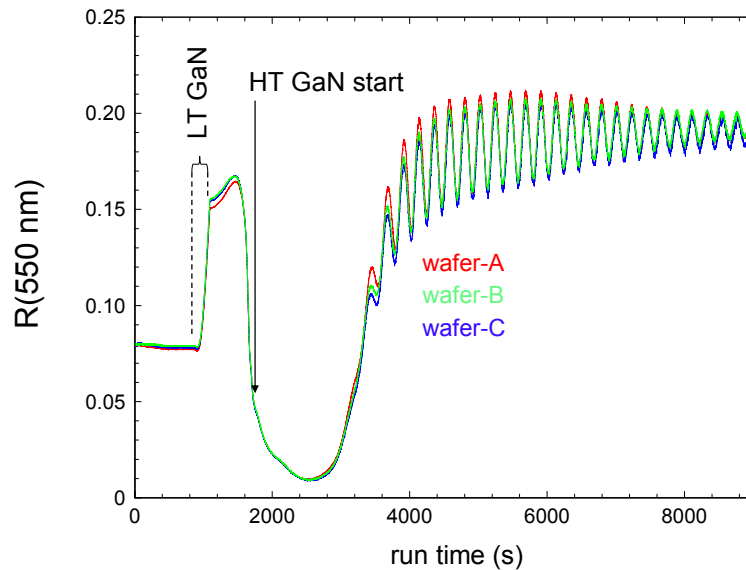


Fig. 6. Individual wafer reflectance (550 nm) during GaN/sapphire MOCVD

A test of the UVV-ECP temperature during growth of an InGaN multi-quantum well (MQW) structure is shown in Fig. 7. This MQW structure consist of five thin InGaN layers (2.8 nm) separated by 10 nm GaN layers. In this run the target deposition temperature was 750°C. The true wafer temperature measured by the UVV-ECP was initially 752°C, but an upward temperature drift was observed towards the end of the deposition sequence. Temperature drift during InGaN growth is one problem that can be solved by incorporating the UVV-ECP technology into a closed loop control system.

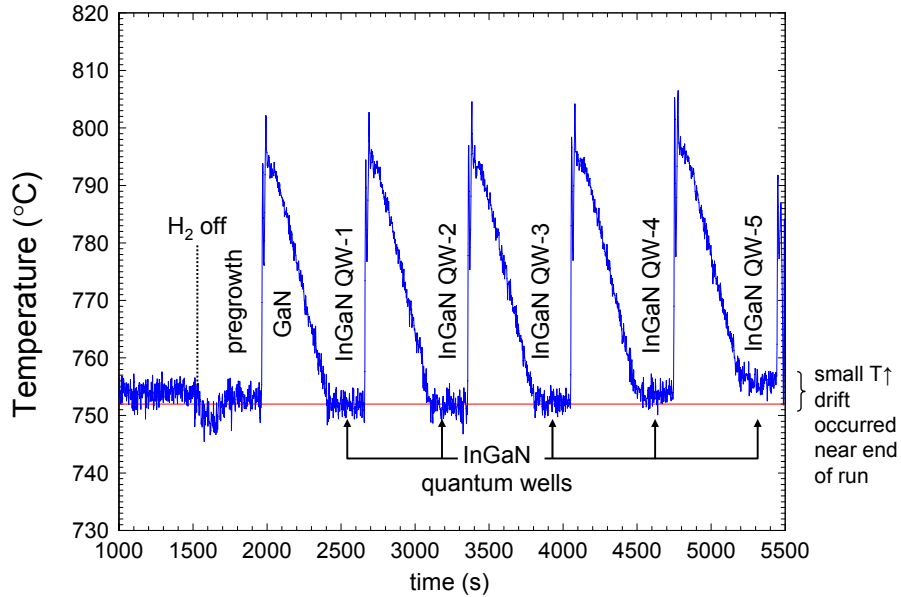


Fig. 7. UVV-ECP Temperature during growth of multi-quantum well InGaN structure in multiwafer D-125 Veeco MOCVD reactor

Among the most important metrics of the system are the signal-to-noise ratios (S/N) for the temperature and reflectance measurements. For the 405 nm channel we are using pulse-counting electronics which is expected to yield shot-noise limited signals. For a given count rate ( $I$ ) and counting time ( $\tau$ ) it is easy to calculate the expected S/N;  $S/N_{rms} = (I\tau)^{1/2}$ . For the 405 nm reflectance channel we have abundant signal, in fact we normally attenuate the light source to yield 1-4 MHz count rate for a sapphire wafer (We limit the maximum count rate to less than 10 MHz because of non-linearities that occur in the photomultiplier (PMT) detector and pulse counting electronics at very high count rates).

By using the measured blackbody calibration curve and the known characteristics of the system we can calculate the expected temperature noise. In the Wein limit the blackbody distribution function [3] reduces to Eqn. 1. Differential analysis of Eq. 1 allows us to derive the approximate temperature noise ( $\Delta T_{rms}$ ), which is given in Eq. 2. This curve is plotted in Fig. 8 for the following conditions;  $\epsilon = 0.8$  (GaN value), 3-wafer average, platen counting time = 1 sec. We also use a typical window transmission of 0.92. For a one-wafer measurement the temperature noise will be  $\sqrt{3}$  larger.

$$S(\text{counts}) = A \cdot \varepsilon \cdot \tau \cdot \exp\left(-\frac{c_2}{\lambda T}\right) \quad (1)$$

$A$  = blackbody calibration factor

$\varepsilon$  = emissivity

$\tau$  = counting time

$c_2 = 1.438 \times 10^7$  nm-deg (2<sup>nd</sup> radiation constant)

$\lambda$  = effective wavelength

$$\Delta T_{rms} \approx \frac{\lambda T^2}{c_2} \sqrt{\frac{\exp(c_2/\lambda T)}{A \cdot \varepsilon \cdot \tau}} \quad (2)$$

Above 1000°C (typical GaN conditions) the temperature noise is well below 0.1°C, which is certainly adequate performance. As the temperature is lowered into the 700-800°C range the temperature noise starts to become significant. This is the temperature range for InGaN alloy deposition, and here the performance of the pyrometer becomes critical. The InGaN emission wavelength has a temperature sensitivity of 1-2 nm/deg, so temperature uncertainties and drift are very important for reproducibility. Near 800°C the system should be useful using a counting time of a few seconds, but near 700°C we may need to time average over 10's of seconds. In the future we will search for ways of improving S/N, such as increasing the effective wavelength.

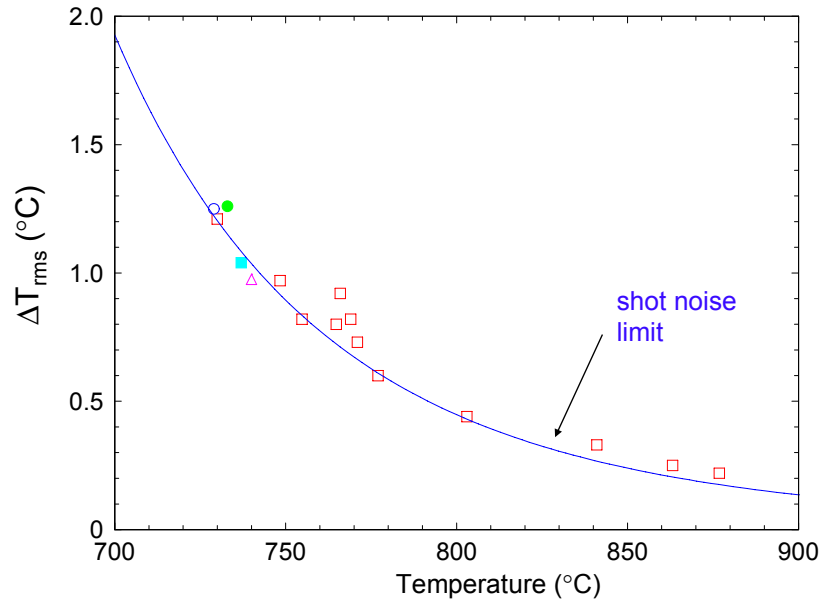


Fig. 8. Theoretical and measured temperature noise (rms) for 1 second integration time, 3-wafer average.

The temperature noise measurements for the InGaN MQW sample shown in Fig. 8 represent the achievement of half of Milestone 1.12. Results during the pre-growth step and the 5 quantum wells (QW) are summarized in Table 1. In the final column, single wafer measurements have been numerically converted to a 3-wafer average by dividing by  $\sqrt{3}$ , which is the expected (and observed) scaling factor for shot-noise limited performance. The average of the first five measurements is  $0.78^\circ\text{C}$ , which meets our target  $< 0.8^\circ\text{C}$ . The final QW temperature drifted just above our target window of  $750 \pm 5^\circ\text{C}$  and is not included in the average.

**Table 1. Temperature noise measurements**

Structure	1-wafer T-noise ( $\sigma$ )	Average Temperature	3-wafer T-noise ( $\sigma$ )
Pre-growth	$1.27^\circ\text{C}$	$754.2^\circ\text{C}$	$0.73^\circ\text{C}$
QW-1	$1.37^\circ\text{C}$	$752.0^\circ\text{C}$	$0.79^\circ\text{C}$
QW-2	$1.48^\circ\text{C}$	$751.6^\circ\text{C}$	$0.85^\circ\text{C}$
QW-3	$1.32^\circ\text{C}$	$752.4^\circ\text{C}$	$0.76^\circ\text{C}$
QW-4	$1.33^\circ\text{C}$	$753.7^\circ\text{C}$	$0.77^\circ\text{C}$
QW-5	$1.25^\circ\text{C}$	$755.7^\circ\text{C}$	$0.72^\circ\text{C}$

Another metric for performance is the degree of correlation between the true wafer temperature (measured by the UVV-ECP) and the InGaN photoluminescence (PL) wavelength. We performed a series of growth runs with the same InGaN multi-quantum well growth recipe, only varying the wafer temperature during the InGaN QW step. As seen in Fig. 9, raising the temperature leads to a reduction in indium incorporation and a strong blue shift in the median PL emission wavelength. The horizontal error bars shown represent the degree of temperature drift that occurred during the MQW sequence. The recipe we used for this data set was not optimized for lower temperature InGaN growth and resulted in broad asymmetric PL spectra for the green samples, which is the reason for using the median (rather than maximum) wavelength metric. From  $723^\circ$  to  $800^\circ\text{C}$  the emission shifts from the green (512 nm) to the near ultraviolet (399 nm) with a slope of  $\sim -1.5 \text{ nm}/^\circ\text{C}$ . It may be fortuitous that this data set is well described by a simple linear function, what is important is the smooth nature of the functional relationship with little apparent scatter ( $r^2 = 0.995$ ). The measured high correlation coefficient meets the 2<sup>nd</sup> portion of Milestone 1.12 ( $r^2 > 0.8$ ). An indirect temperature measurement is expected to exhibit much more scatter and a smaller degree of correlation.

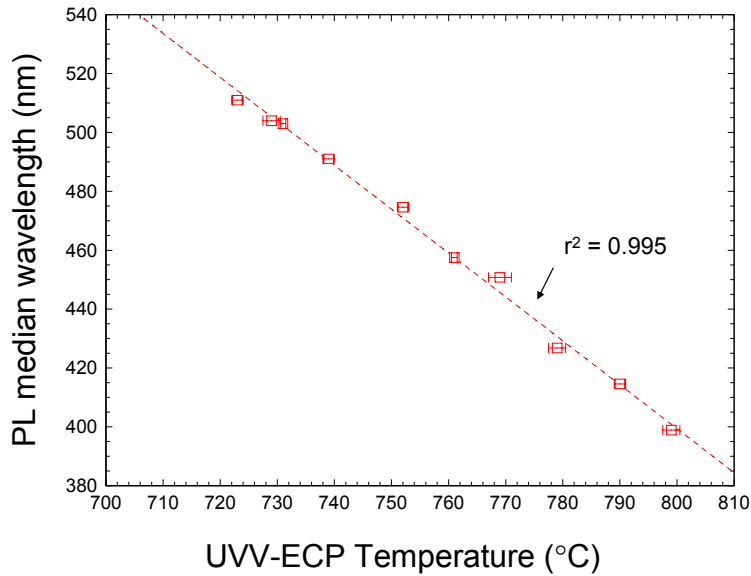


Fig. 9. Correlation between the InGaN median PL wavelength and the true wafer temperature

## 6. Status of the MIR-ECP System

We are developing a MIR-ECP prototype using near-normal incidence (2-4°) geometry and our “standard” emissivity-correction scheme (see Fig. 10.). The key component is a thermoelectrically-cooled HgCdZnTe photovoltaic detector sensitive to MIR radiation. Because the GaN/sapphire interference oscillations at ~ 7.5 microns are too slow to serve as a useful growth rate monitor, we are also planning to include a collinear visible or near-IR (550-900 nm) reflectance channel. Because fiberoptic cables with good transmission properties in the visible and mid-IR are not available we must design a compact system that can be mounted directly on the reactor viewport. We have identified two options for our reflectance source; a 5 watt quartz-halogen bulb, and a 9 watt ceramic IR source. The tradeoffs are the amount of vis-NIR versus MIR emission from the two sources.

We have tested a variety of collection optics to be used with the IR detector. Using simple lenses at magnifications greater than 4X leads to poor image quality, so we are currently using a lower magnification (3X) BaF<sub>2</sub> lens. In the future, if we need more signal we will reexamine this issue. System calibration against a blackbody source yields a nearly perfect blackbody response curve with an effective wavelength of 7.8 microns. With the current optical configuration and filter we can easily meet expected temperature noise metric. The current filter bandwidth is 800 cm<sup>-1</sup>, but may need to decrease this to ~ 300 cm<sup>-1</sup> to avoid gas-phase NH<sub>3</sub> absorption. This will decrease the signal by 4X, but it looks like we can lose this amount of signal and still meet the noise metric. We are on track to meet milestone 2.11, but many technical issues were not fully optimized or investigated to our complete satisfaction. For example, even at low (3X) magnification the detector is seeing a small signal 0.3-0.5% outside of expected field of view, possibly from aberrations in optics, or scattering within the detector module.

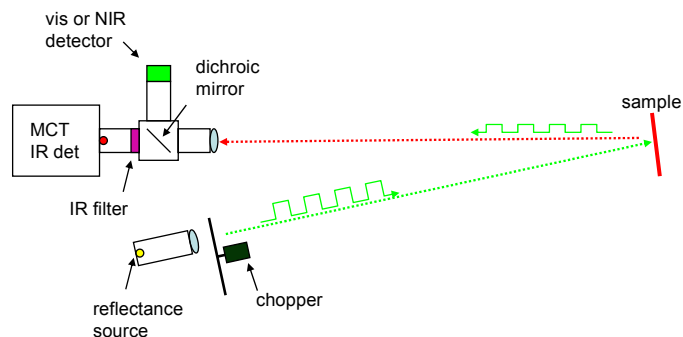


Fig. 10. First prototype of MIR-ECP system to be installed on our research reactor

We have been collecting the required optical and mechanical components but have not had time to test the “self-reflectance” emissivity correction method (i.e. see Fig. 11). This method (proposed by Bill Breiland, Sandia) is potentially more accurate than our standard method, because it uses the samples own thermal emission signal to measure the reflectance (and therefore emissivity). The standard method is sensitive to drifts in intensity of the reflectance source, while the self-reflectance method does not suffer from this effect. Both methods still rely on the absolute calibration of one measurement, usually measurement of the reflectance of a known standard.

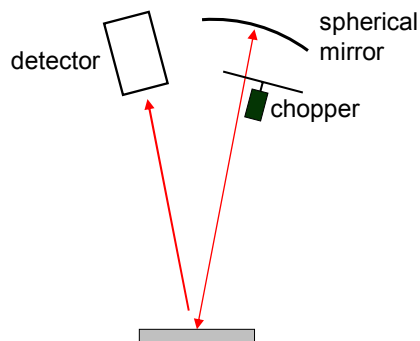


Fig. 11. Schematic of Self-Reflectance method of emissivity-correction

## 7. Milestone Summary

Project Milestones are shown in the table below, with green indicating completion, and yellow indicating on schedule (for Budget Period 1). Milestone 1.11 was achieved by the target date. The first half of Milestone 1.12 (temperature noise metric) was achieved by the target date, while the second half (PL-temperature correlation) was approximately one month late due to the time required to grow the films and perform the PL analysis. We project that we will complete Milestone 2.11 by the target date (or within a short time thereafter).

- Complete Milestone
- On Schedule

Year 1	Completion Time
Milestone 1.11 Design and install 1 <sup>st</sup> generation UVV-ECP for multiwafer InGaN MOCVD system.	3/31/05
Milestone 1.12 Evaluate performance of 1 <sup>st</sup> generation UVV-ECP for InGaN conditions: <ul style="list-style-type: none"> <li>▪ Temperature noise (rms) &lt; 0.8 degrees at temperature of 750 ± 5 °C at 1 Hz bandwidth and 3 wafer average.</li> <li>▪ Correlation Coefficient (r<sup>2</sup>) &gt; 0.8 for PL wavelength vs. temperature curve.</li> </ul>	6/30/05
Milestone 2.11 Develop prototype MIR-ECP for research RDR (CVD1).	9/30/05
Year 2	
Milestone 2.21 Evaluate and refine mid-IR ECP hardware.	12/31/05
Milestone 1.21 Explore and develop sensitivity improvements for UVV-ECP for 2 <sup>nd</sup> generation. <ul style="list-style-type: none"> <li>▪ New filter set to increase UVV-ECP signal by &gt;3x (if allowed by opacity issues)</li> </ul>	12/31/05
Milestone 2.22 Install prototype MIR-ECP on multiwafer InGaN MOCVD reactor.	3/31/06
Milestone 2.23 Evaluate and compare performance of 2 <sup>nd</sup> generation UVV-ECP and MIR-ECP. <ul style="list-style-type: none"> <li>▪ MIR-ECP temperature noise (rms) &lt;0.3 degrees over 700-800 °C range at 1Hz bandwidth and 3 wafer average.</li> <li>▪ UVV-ECP temperature noise (rms) &lt;0.4 degrees at temperature of 750 ± 5 °C at 1 Hz bandwidth and 3 wafer average.</li> <li>▪ Demonstrate a 2X improvement in LED wavelength targeting as compared to our previous results of an average deviation of 6nm with a maximum deviation of 11 nm to an average deviation of ≤ 3 nm, and a maximum deviation ≤ 6 nm for a target wavelength &gt; 500 nm</li> </ul>	9/30/06

## 8. References

1. J.A. Simmons et al, “Final Report on Grand Challenge LDRD Project: A Revolution in Lighting-Building the Science and Technology Base for Ultra-Efficient Solid State Lighting”, Technical Report, Sandia National Laboratories, Albuquerque, NM 87185, SAND2004-2365.
2. W.G. Breiland, “Reflectance-Correcting Pyrometry in Thin Film Deposition Applications”, Technical Report, Sandia National Laboratories, Albuquerque, NM 87185, SAND2003-1868.
3. D.P. DeWitt and G.D. Nutter, eds. “Theory and Practice of Radiation Thermometry”, John Wiley and Sons, Inc. 1988.

## Distribution

4	MS 0601	J. R. Creighton
1	MS 0601	D. D. Koleske
1	MS 0601	R. M. Biefeld
2	MS 9018	Central Technical Files, 8944
2	MS 0899	Technical Library, 4536